ESC European Society of Cardiology

Cardiovascular Research (2017) **113**, 1148–1160
doi:10.1093/cvr/cvx100

Diabetic *db/db* mice do not develop heart failure upon pressure overload: a longitudinal *in vivo* PET, MRI, and MRS study on cardiac metabolic, structural, and functional adaptations

Desiree Abdurrachim[1†], Miranda Nabben[1,2†], Verena Hoerr[3,4], Michael T. Kuhlmann[5], Philipp Bovenkamp[3], Jolita Ciapaite[6], Ilvy M.E. Geraets[2], Will Coumans[2], Joost J.F.P. Luiken[2], Jan F.C. Glatz[2], Michael Schäfers[5,7,8], Klaas Nicolay[1], Cornelius Faber[3], Sven Hermann[5,7], and Jeanine J. Prompers[1]*

[1]Department of Biomedical Engineering, Biomedical NMR, Eindhoven University of Technology, PO Box 513, 5600 MB Eindhoven, The Netherlands; [2]Department of Genetics and Cell Biology, CARIM School for Cardiovascular Diseases, Maastricht University, Maastricht, The Netherlands; [3]Department of Clinical Radiology, University Hospital of Münster, Münster, Germany; [4]Institute of Medical Microbiology, Jena University Hospital, Jena, Germany; [5]European Institute for Molecular Imaging-EIMI, Münster, Germany; [6]Department of Pediatrics and Systems Biology Center for Energy Metabolism and Ageing, Center for Liver, Digestive and Metabolic Diseases, University of Groningen, University Medical Center Groningen, Groningen, The Netherlands; [7]Cells-in-Motion Cluster of Excellence, University of Münster, Münster, Germany; and [8]Department of Nuclear Medicine, University of Münster, Münster, Germany

Received 30 September 2016; revised 9 March 2017; editorial decision 6 April 2017; accepted 23 May 2017; online publish-ahead-of-print 26 May 2017

Time for primary review: 37 days

Aims Heart failure is associated with altered myocardial substrate metabolism and impaired cardiac energetics. Comorbidities like diabetes may influence the metabolic adaptations during heart failure development. We quantified to what extent changes in substrate preference, lipid accumulation, and energy status predict the longitudinal development of hypertrophy and failure in the non-diabetic and the diabetic heart.

Methods and results Transverse aortic constriction (TAC) was performed in non-diabetic (*db/+*) and diabetic (*db/db*) mice to induce pressure overload. Magnetic resonance imaging, ^{31}P magnetic resonance spectroscopy (MRS), ^{1}H MRS, and ^{18}F-fluorodeoxyglucose-positron emission tomography (PET) were applied to measure cardiac function, energy status, lipid content, and glucose uptake, respectively. *In vivo* measurements were complemented with *ex vivo* techniques of high-resolution respirometry, proteomics, and western blotting to elucidate the underlying molecular pathways. In non-diabetic mice, TAC induced progressive cardiac hypertrophy and dysfunction, which correlated with increased protein kinase D-1 (PKD1) phosphorylation and increased glucose uptake. These changes in glucose utilization preceded a reduction in cardiac energy status. At baseline, compared with non-diabetic mice, diabetic mice showed normal cardiac function, higher lipid content and mitochondrial capacity for fatty acid oxidation, and lower PKD1 phosphorylation, glucose uptake, and energetics. Interestingly, TAC affected cardiac function only mildly in diabetic mice, which was accompanied by normalization of phosphorylated PKD1, glucose uptake, and cardiac energy status.

Conclusion The cardiac metabolic adaptations in diabetic mice seem to prevent the heart from failing upon pressure overload, suggesting that restoring the balance between glucose and fatty acid utilization is beneficial for cardiac function.

Keywords Heart failure • Pressure overload • Diabetes • Substrate metabolism • *In vivo* imaging techniques

* Corresponding author. Tel: +31 402473128, E-mail: j.j.prompers@tue.nl

† The first two authors contributed equally to the study.

1. Introduction

Cardiac metabolic remodelling is proposed to be an important contributor to the development of heart failure.[1] It is generally accepted that the transition process towards heart failure is accompanied by a shift in cardiac substrate preference, with a greater reliance on glucose utilization and a concomitant suppression of fatty acid oxidation (FAO).[2–5] This metabolic shift seems to precede the onset of cardiac dysfunction.[6] In addition, the failing heart is characterized by an imbalance between energy supply and demand leading to a cardiac energy deficit, i.e. a lower phosphocreatine-to-ATP ratio (PCr/ATP).[7] The myocardial PCr/ATP ratio has been identified as a strong predictor of mortality in heart failure patients.[8] It is currently not clear, however, whether the metabolic shift towards increased glucose utilization upon heart failure is a beneficial adaptive mechanism, and whether it is a cause or consequence of the reduced cardiac energetic status.

Type 2 diabetes patients have a 2.5 times higher risk of heart failure compared with subjects without diabetes.[9] The diabetic heart almost exclusively (90–100%) relies on FAO and has lost the flexibility to switch from FAO to glucose utilization.[10] Moreover, the diabetic heart has a decreased energy status[11] and an impaired function.[12] Hence, the virtually complete reliance on FAO is potentially detrimental for the diabetic heart, and a possible shift from FAO towards glucose utilization upon heart failure may thus be a beneficial adaptation. In the non-diabetic condition, there are indeed indications that increased glucose utilization could be favourable,[13–15] although it has also been reported that increased FA utilization is beneficial[3,16,17] and that reduced FAO can lead to exacerbated cardiac dysfunction[18–21] (reviewed in[22]). However, as the metabolic phenotype of the diabetic heart differs from that of the normal heart, it remains to be elucidated whether high FA utilization in the diabetic heart is beneficial in assisting the diabetic heart to cope with conditions promoting heart failure. Of note, this could shed light on the 'obesity paradox', i.e. the phenomenon that the prognosis for obese heart failure patient is better than that for non-obese heart failure patients.[23]

To investigate how changes in cardiac substrate preference predict the development of heart failure, an *in vivo* longitudinal study setting is crucial to allow studying the time course of changes in cardiac metabolism and energetics in relation to the decline in cardiac function. After all, evidence for a link between heart failure and changes in cardiac metabolism largely originates from *ex vivo* studies using isolated perfused hearts, and such studies cannot fully mimic the *in vivo* condition. The diabetic heart, for example, is exposed to a hyperglycemic, hyperlipidemic, and hyperinsulinemic environment, which will affect the choice of substrates.[10] Furthermore, the type and concentration of substrates may change during the development of heart failure, which is difficult to address in *ex vivo* studies.

Here, we aim to quantify the cardiac metabolic, structural, and functional changes during heart failure progression in non-diabetic and diabetic mice *in vivo* in a longitudinal study design and investigate how the metabolic profile of the diabetic heart is related to the cardiac metabolic and structural remodelling upon pressure overload (as a model of non-ischemic cardiomyopathy). Pressure overload was induced by transverse aortic constriction (TAC) surgery. Non-invasive magnetic resonance imaging (MRI), ^{31}P magnetic resonance spectroscopy (MRS), ^{1}H MRS, and ^{18}F-fluorodeoxyglucose positron emission tomography (^{18}F-FDG–PET) were applied to measure cardiac function, energy status, lipid content, and glucose uptake, respectively, at baseline and 1, 5, and 12 weeks post-TAC. The *in vivo* data were complemented with measurements of *ex vivo* mitochondrial oxidative capacity and expression levels of proteins involved in mitochondrial oxidative phosphorylation, tricarbocylic acid cycle, fatty acid β-oxidation, and hypertrophic signalling pathways. Our results show that heart failure development in non-diabetic mice correlated with increased protein kinase D-1 (PKD1) phosphorylation and increased myocardial FDG uptake, which preceded the decrease in cardiac energy status. Furthermore, we show that the cardiac metabolic adaptations and signalling in diabetic mice seem to prevent the heart from failing upon pressure overload.

2. Methods

2.1 Animals

Male non-diabetic (*db*/+) and diabetic (*db*/*db*) C57BL/Ks mice (10 weeks of age) were purchased from Charles River. The animals were housed in a specific pathogen-free animal facility of Eindhoven University of Technology in individually ventilated cages and in the conventional facility of Münster University, under controlled temperature (23 °C) and humidity (50%) with a 12:12-h dark–light cycle. The mice had ad libitum access to water and food (5K52 LabDiet; 22 kcal% protein, 16 kcal% fat, 62 kcal% carbohydrates). Three different sets of animals were used: (i) for *in vivo* MRI and ^{31}P MRS measurements in Eindhoven, The Netherlands; (ii) for *in vivo* MRI, ^{1}H MRS, and PET measurements in Münster, Germany; (iii) for baseline *ex vivo* high-resolution respirometry, proteomics, and western blot analyses. Animals (sets 1 and 2) underwent TAC surgery (needle size: 27 G) to induce pressure overload, as described previously.[24] To follow the progression of cardiac hypertrophy and failure, the PET and/or MR measurements were performed before, 1, 5, and 12 weeks post-TAC. The surgery and the measurements were performed under isoflurane anaesthesia (induction: 3–4%, maintenance: 2–3% for surgery; 1–2% for measurements, in 0.2 l/min medical air and 0.2 l/min O_2). Analgesic buprenorphine (0.1 mg/kg) was administered subcutaneously 12 h before the surgery and repeated daily for 3 days. The animals were sacrificed by cervical dislocation under isoflurane anaesthesia, after the measurements at 12 weeks post-TAC (sets 1 and 2) or at baseline (set 3). The heart was excised and half of it was used immediately for isolation of mitochondria for high resolution respirometry and proteomics measurements. The other part was frozen in liquid nitrogen for western blotting. All procedures conformed to the Directive 2010/63/EU of the European Parliament, and were approved by the Animal Experimental Committees of Maastricht University (The Netherlands) and The North Rhine-Westphalia Agency for Nature, Environment, and Consumer Protection (Landesamt für Natur, Umwelt und Verbraucherschutz Nordrhein-Westfalen-LANUV, Germany).

2.2 MRI and MRS

Cardiac-triggered and respiratory-gated cine MRI, ^{1}H MRS, and ^{31}P MRS were performed to measure cardiac function, lipid content, and energy status, respectively. Additionally, to determine the severity of the TAC surgery, blood flow through right and left carotid arteries was measured using a flow velocity encoded MRI sequence. Details of the MRI/MRS and all other experimental methods are provided in the Supplementary material online.

2.3 Positron emission tomography

PET measurements were performed after a 12–13 h overnight fast. The acquisition was performed 1 h after ^{18}F-FDG injection (~10 MBq in 100 µl), for 15 min.

2.4 Fasting plasma glucose

Plasma glucose levels were measured after a 4 h fast in one drop of blood using a Glucose-201 glucose meter (HemoCue, Ängelholm, Sweden).

2.5 High-resolution respirometry

A two-channel high-resolution Oxygraph-2k (Oroboros, Innsbruck, Austria) was used to measure oxygen consumption rates in isolated cardiac mitochondria using (i) pyruvate plus malate or (ii) palmitoyl-CoA plus L-carnitine plus malate as substrates.

2.6 Targeted quantitative mitochondrial proteomics

Fifty-four mitochondrial proteins involved in substrate transport, FAO, and the TCA cycle were quantified in isolated mitochondria using isotopically labelled standards (^{13}C-labelled lysines and arginines).

2.7 Western blot analyses

Western blot analyses were performed in cardiac muscle homogenates to determine the expression of phosphorylated acetyl-CoA carboxylase (p-ACC) (Ser 79), ACC, p-mechanistic target of Rapamycin (p-mTOR) (Ser 2448), p-extracellular signal-regulated kinase (p-ERK) (Thr 202), p-Ca^{2+}/calmodulin-dependent protein kinase II (p-CAMKII) (Thr 286), p-PKD (Ser 916), PKD, p-Troponin I (Ser 23/24), and p-histone deacetylase-5 (p-HDAC5) (Ser 498). The relative values were corrected to glyceraldehyde 3-phosphate dehydrogenase (GAPDH) expression levels and normalized with respect to baseline controls.

2.8 RNA expression analyses

RNA expression analyses were performed in cardiac muscle homogenates to determine the expression of atrial natriuretic factor (ANF) and brain natriuretic peptide (BNP). The quantitative polymerase chain reaction (PCR) values were corrected to Cyclophilin A expression levels and normalized with respect to baseline controls.

2.9 Statistics

Data are presented as means ± SD. Statistical significance of genotype (non-diabetic and diabetic mice) and time (baseline, 1, 5, and 12 weeks post-TAC) effects were assessed by applying a two-way analysis of variance in the IBM SPSS 21.0 (SPSS Inc., Chicago, IL, USA). The general genotype effects and the general time effects were reported only when the interaction term between genotype and time was not significant. In case of a significant general effect of time, Fisher's least significant difference (LSD) post-hoc tests were performed to identify differences between different time points. In case the interaction term between genotype and time was significant, the simple main effects between genotypes at each time point and within the same genotype between different time points were evaluated using Estimated Marginal Means (EMMEANS). Correlations between parameters were assessed using a Pearson's correlation. Statistical significance was set at $P < 0.05$.

3. Results

3.1 Animal characteristics

Physiological characteristics of the mice are shown in *Table S1*, see Supplementary material online. Body weight of the diabetic mice was 1.5–1.8 times higher than that of non-diabetic mice at all time points ($P < 0.001$). Plasma glucose levels were three to five times higher in diabetic than in non-diabetic mice at all time points ($P < 0.05$). At 12 weeks post-TAC, wet lung weights were lower in diabetic than in non-diabetic mice ($P = 0.016$). In non-diabetic mice, wet lung weights were higher at 12 weeks post-TAC compared with baseline ($P = 0.041$, respectively), indicating pulmonary congestion.

3.2 Post-surgical mortality

A total of 36 diabetic mice and 26 non-diabetic mice were involved in the study. The TAC surgical procedure appeared to be less tolerated by the diabetic mice; 18 diabetic mice compared with 3 non-diabetic mice died within a few hours up to 2 days after surgery. After this critical time, the mortality rate was 33% and 14% at 12 weeks post-TAC for non-diabetic and diabetic mice, respectively (data from Set 1 animals). Mortality rates in Set 2 animals were higher compared with Set 1 animals, especially for diabetic mice, which is likely related to the more intensive experimental protocol involving overnight fasting prior to PET measurements, followed by two sessions of anaesthesia within a 3-day period.

3.3 TAC affected left ventricular mass and function severely in non-diabetic mice, but only mildly in diabetic mice

Blood flow velocities in right and left carotid arteries indicate the degree of constriction of the aortic arch by the TAC procedure. At 1 week after TAC, blood flow was similarly increased in the right and decreased in the left carotid arteries in non-diabetic and diabetic mice (see Supplementary material online, *Figure S1*), indicating that the pressure overload achieved after surgery was comparable between genotypes. Furthermore, blood flow velocities in the carotids remained similar between non-diabetic and diabetic mice at 5 weeks post-TAC (see Supplementary material online, *Figure S1*; data at 12 weeks post-TAC not available), indicating no differences in band integrity between groups. In non-diabetic mice, left ventricular (LV) mass (*Figure 1A, B*) progressively increased from a 37% increase with respect to baseline at 1 week post-TAC ($P < 0.001$ vs. baseline) to a 92% increase at 12 weeks post-TAC ($P < 0.001$ vs. baseline). Interestingly, the increase in LV mass was less pronounced in diabetic mice, in which LV mass only increased by 20% at 1-week post-TAC ($P = 0.038$ vs. baseline) and by 52% at 12 weeks post-TAC ($P < 0.001$ vs. baseline). At 12 weeks post-TAC, LV mass was 28% lower in diabetic as compared with non-diabetic mice ($P < 0.001$).

In non-diabetic mice, the progressive hypertrophy upon TAC was accompanied by increases in end-diastolic and end-systolic volumes (ESV) over time (*Figure 1C, D*), resulting in a 30% reduction in stroke volume (SV) at 1 week post-TAC ($P < 0.001$ vs. baseline), which was maintained until 12 weeks post-TAC (*Figure 1E*). Similarly, in non-diabetic mice, ejection fraction (EF) progressively decreased after TAC, from a 36% decrease with respect to baseline at 1 week post-TAC ($P < 0.001$ vs. baseline) to a 47% decrease at 12 weeks post-TAC ($P < 0.001$ vs. baseline).

In contrast, in diabetic mice, ESV and SV were not affected by TAC (*Figure 1D, E*). Moreover, in diabetic mice, EF was preserved at 1 and 12 weeks post-TAC ($P = 0.101$ and 0.157 vs. baseline, respectively), while it was slightly decreased at 5 weeks post-TAC (16%, $P = 0.030$ vs. baseline).

Peak filling rate, a measure of cardiac diastolic function, was significantly higher in diabetic mice compared with non-diabetic mice at 5 weeks post-TAC ($P = 0.001$; *Figure 1G*).

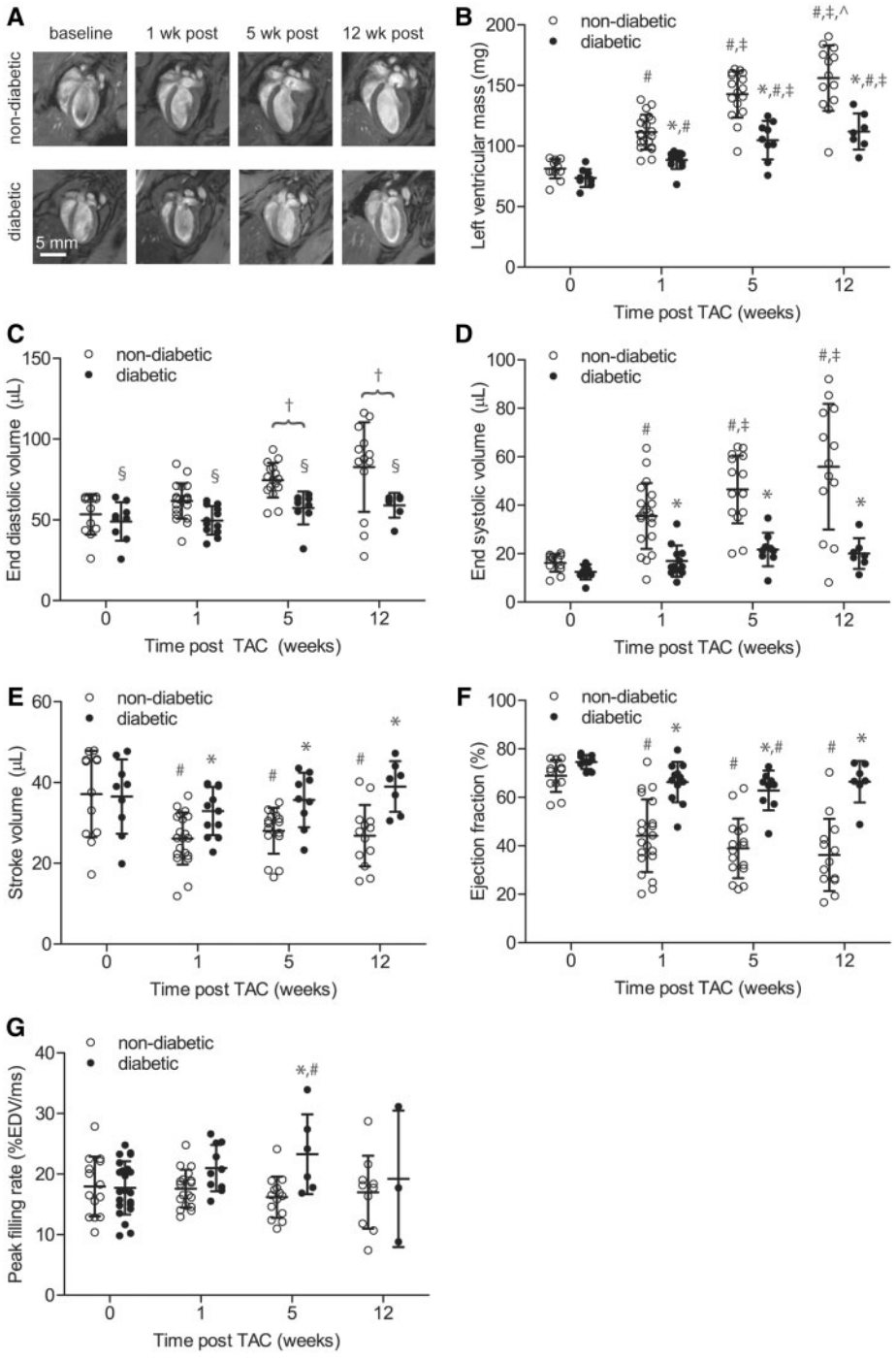

Figure 1 TAC affected LV mass and function severely in non-diabetic mice, but only mildly in diabetic mice. (*A*) Representative MR images of four-chamber long axis views, (*B*) LV mass, and (*C–G*) cardiac function parameters derived from MRI. Data are means ± SD (n = 12–20 for non-diabetic mice, n = 7–12 for diabetic mice). *P < 0.05 vs. non-diabetic mice at the same time point, $^{\#}P$ < 0.05 vs. baseline for the same genotype, $^{\ddagger}P$ < 0.05 vs. 1 week post-TAC for the same genotype, $^{\wedge}P$ < 0.05 vs. 5 weeks post-TAC for the same genotype, $^{\dagger}P$ < 0.05 vs. baseline independent of genotype, and $^{\S}P$ < 0.05 vs. non-diabetic mice independent of time.

3.4 Myocardial FDG uptake was lower in diabetic mice, but increased in both non-diabetic and diabetic mice upon TAC

Myocardial glucose uptake was measured *in vivo* in the LV using ^{18}F-FDG–PET (*Figure 2A*). At baseline, FDG uptake was 44% lower in diabetic mice than in non-diabetic mice (P = 0.006). In non-diabetic mice, FDG uptake increased 2.2-fold at 1 week post-TAC (P < 0.001 vs. baseline) and remained increased at 5 weeks post-TAC (2.5-fold; P < 0.001 vs. baseline; *Figure 2B*). Interestingly, the increased myocardial FDG uptake in the non-diabetic mice strongly correlated with changes in

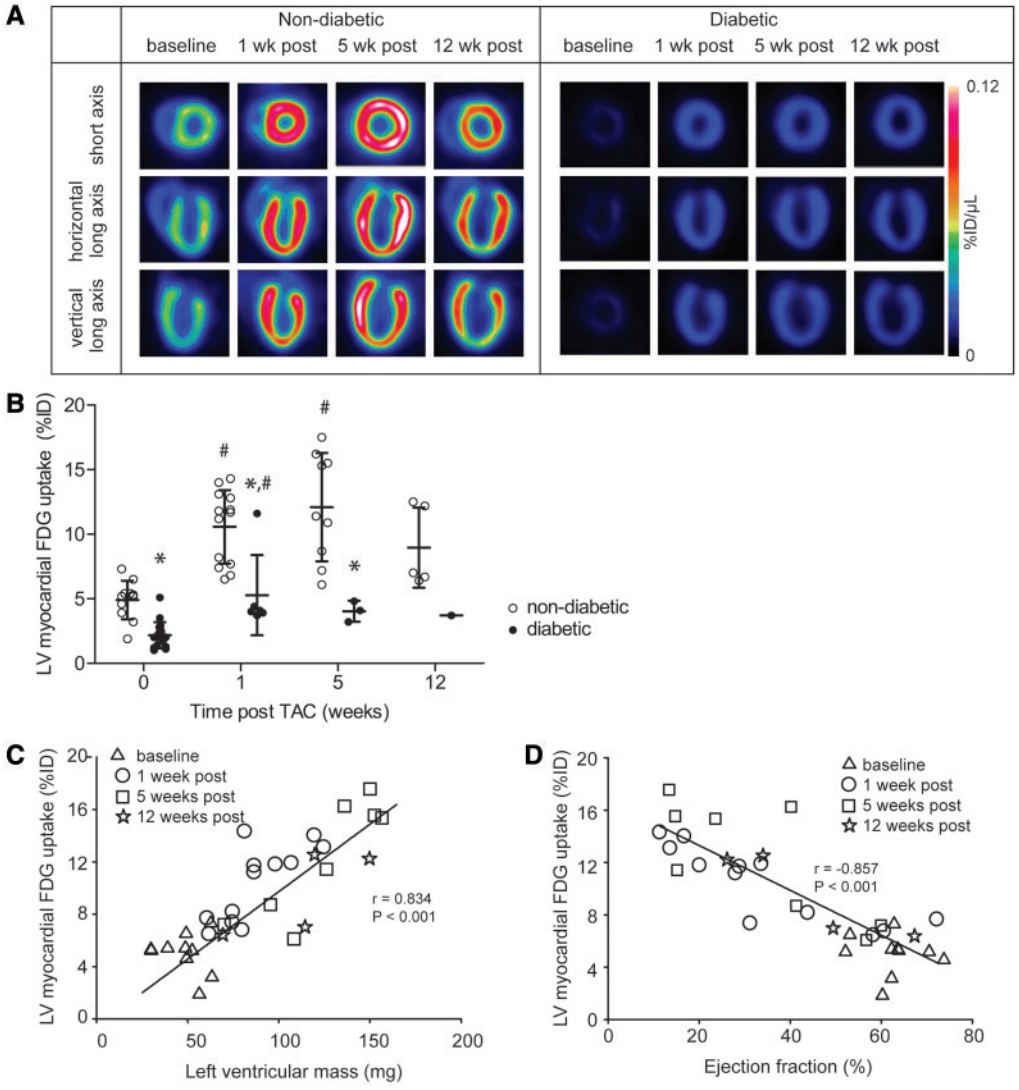

Figure 2 TAC increased myocardial FDG uptake in non-diabetic and diabetic mice, but the levels were lower in diabetic mice. (*A*) ^{18}F-FDG PET images from 3 cardiac axis views. Color intensity represents the level of ^{18}F-FDG uptake in percentage of injected dose (%ID) per µl of myocardial volume. (*B*) Quantification of total LV myocardial ^{18}F-FDG uptake. Data are means ± SD (n = 5–13 for non-diabetic mice, n = 1–17 for diabetic mice). Data of diabetic mice at 12 weeks post-TAC was excluded from statistical analysis. *P < 0.05 vs. non-diabetic mice at the same time point, $^{\#}P$ < 0.05 vs. baseline for the same genotype. Correlations between (*C*) myocardial FDG uptake and LV mass and (*D*) myocardial FDG uptake and EF (data are from non-diabetic mice; 34 points).

LV mass and EF (r = 0.834 and r = -0.857, respectively; P < 0.001; *Figure 2C, D*). Furthermore, the myocardial FDG uptake in the non-diabetic mice also correlated with SV (r = -0.526, P = 0.001) and CO (r = -0.565, P = 0.001). In diabetic mice, FDG uptake increased at 1 week post-TAC compared with baseline (2.4-fold; P = 0.011; *Figure 2B*). After TAC, FDG uptake in diabetic mice remained lower than in non-diabetic mice, but reached a level that was similar to the baseline level of non-diabetic mice. Similar results were obtained when FDG uptake was normalized to LV mass (see Supplementary material online, *Figure S2*).

3.5 *In vivo* myocardial lipid content was higher in diabetic mice but not affected by TAC

Myocardial lipid content was measured in the myocardial septum using ^{1}H MRS (*Figure 3A*), by quantifying the triglyceride (TG) methylene peak relative to the water signal (*Figure 3B*). Myocardial TG levels were ∼50% higher in diabetic mice compared with non-diabetic mice (general genotype effect P < 0.001), but were not affected by TAC in either genotype (*Figure 3C*). Similarly, three other signals associated with TG (TG olefinic, β-methylene, and methyl peaks) were significantly higher in diabetic mice compared with non-diabetic mice (general genotype effects P = 0.003, P = 0.001, and P = 0.052, respectively; data not shown).

3.6 Cardiac energy status decreased in non-diabetic mice upon TAC, while low baseline cardiac energy status in diabetic mice recovered after TAC

^{31}P MRS of the LV (*Figure 4A*) was used to quantify the myocardial PCr/ATP ratio as a measure of cardiac energy status *in vivo* (*Figure 4B, C*). At baseline, the PCr/ATP ratio was 41% lower in diabetic mice than in non-

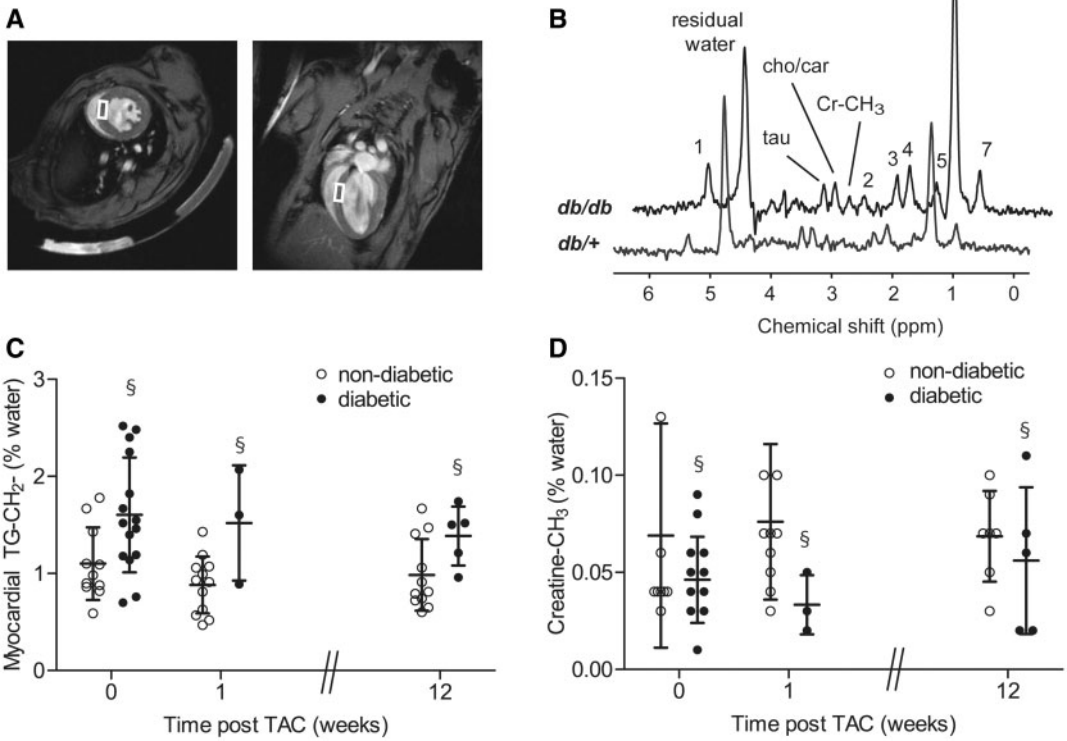

Figure 3 Myocardial lipid content was higher in diabetic mice, while total myocardial creatine content was lower in diabetic mice. (*A*) Positioning of the $1 \times 2 \times 2\,mm^3$ voxel used for ^1H MRS. (*B*) Representative cardiac ^1H MR spectra at baseline, showing peaks originating from taurine, choline/carnitine, creatine-CH_3, and 7 peaks associated with TG protons (indicated in bold): (1) C**H** = C**H**; (2) -CH = CH-C**H$_2$**-CH = CH-; (3) -C$_\alpha$**H$_2$**COO-; (4) -C**H$_2$**-CH = CH-C**H$_2$**-; (5) -C$_\beta$**H$_2$**CH$_2$COO-; (6) -C**H$_2$**-; (7) -C**H$_3$**. (C) Myocardial TG-CH_2 content, and (D) total creatine content. Data are means ± SD (n = 11–12 for non-diabetic mice, n = 3–15 for diabetic mice). $^{\S}P < 0.05$ vs. non-diabetic mice independent of time.

diabetic mice ($P < 0.001$; *Figure 4D*). TAC did not affect the PCr/ATP ratio at 1 and 5 weeks post-TAC, but at 12 weeks post-TAC the PCr/ATP ratio was significantly reduced in non-diabetic mice ($P = 0.022$ vs. baseline) while it was increased in diabetic mice ($P = 0.019$ vs. baseline; *Figure 4D*). In line with the lower cardiac energy status in diabetic mice, total creatine levels as measured by ^1H MRS were lower in diabetic mice compared with non-diabetic mice (general genotype effect $P = 0.038$; *Figure 3D*).

3.7 TAC decreased cardiac mitochondrial oxidative capacity, but FAO capacity was better maintained in diabetic mice

We measured mitochondrial oxidative capacity in isolated heart mitochondria of non-diabetic and diabetic mice at baseline and at 12 weeks post-TAC. At baseline, mitochondrial respiratory capacity for a glucose-derived substrate (i.e. pyruvate plus malate) was similar between non-diabetic and diabetic mice (*Figure 5A, B*). However, when using a FA substrate to fuel mitochondrial respiration (i.e. palmitoyl-CoA plus carnitine plus malate) state 3 and uncoupled respiratory capacity each were higher in diabetic mice than in non-diabetic mice (general genotype effect $P < 0.001$ for state 3, $P = 0.025$ for uncoupled state; *Figure 5D, E*). At 12 weeks post-TAC, there was a genotype-independent decrease in state 3 and uncoupled respiratory capacity on the glucose-derived substrate compared with baseline (general time effect of ~25%; $P = 0.001$ for state 3, $P = 0.013$ for uncoupled state; *Figure 5A, B*). TAC similarly resulted in a genotype-independent decrease in state 3 respiratory capacity on the FA substrate (general time effect $P = 0.001$; *Figure 5D*), but respiration remained higher in diabetic mice than in non-diabetic mice (general genotype effect $P < 0.001$; *Figure 5D*). Interestingly, while uncoupled respiratory capacity of non-diabetic mice for the FA substrate was 35% lower at 12 weeks post-TAC compared with baseline ($P = 0.001$), uncoupled respiratory capacity of diabetic mice was not affected by TAC ($P = 0.362$; *Figure 5E*). State 4 respiration was similar between non-diabetic and diabetic mice for both substrates, and unaffected by TAC (*Figure 5C, F*).

3.8 TAC lowered levels of mitochondrial proteins involved in FAO, TCA cycle and oxidative phosphorylation similarly in non-diabetic and diabetic mice

To investigate which steps in the mitochondrial metabolic pathway account for the decreased state 3 respiration upon TAC, we performed proteomics analysis in isolated heart mitochondria at baseline and at 12 weeks post-TAC (*Figure 6*). We measured the levels of mitochondrial proteins involved in β-oxidation (*Figure 6A*), TCA cycle (*Figure 6B*), and oxidative phosphorylation (*Figure 6C*). Proteomics analyses showed that TAC collectively reduced the expression of mitochondrial proteins involved in β-oxidation [carnitine palmitoyl transferase-2 (CPT2),

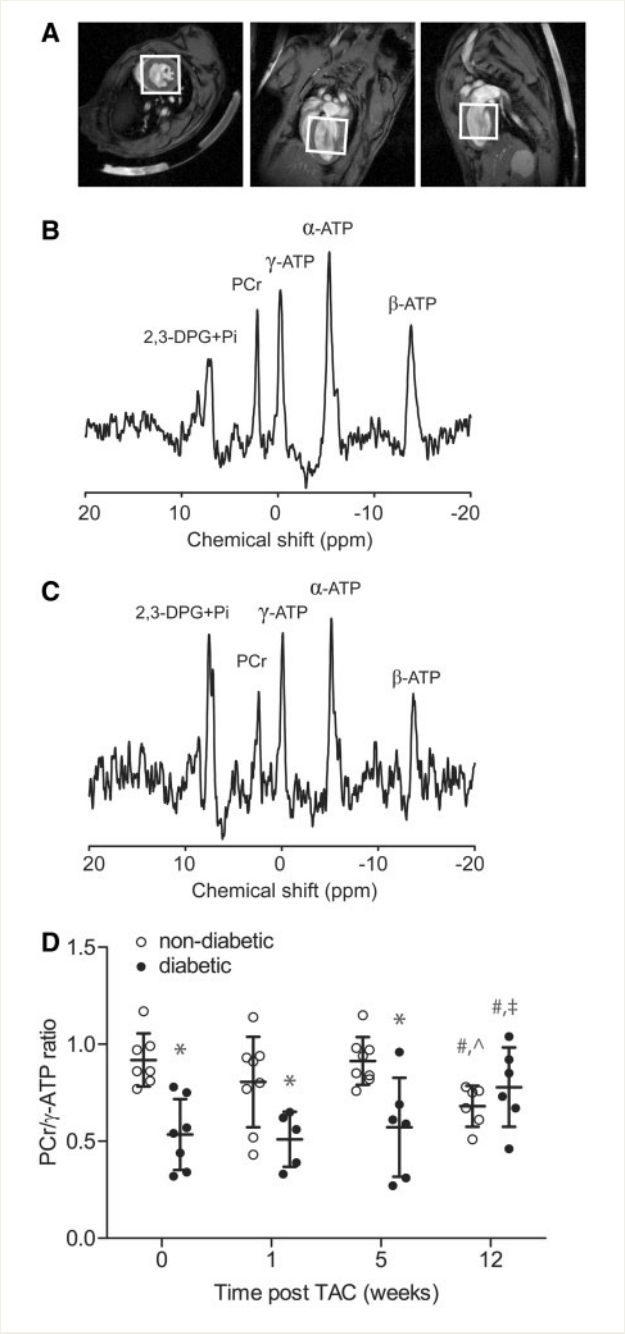

Figure 4 TAC decreased cardiac energy status in non-diabetic mice, while low baseline cardiac energy status in diabetic mice recovered after TAC. (*A*) Positioning of the voxel (typically 5^3–7^3 mm^3, enclosing the left ventricle) used for ^{31}P MRS. Representative cardiac ^{31}P MR spectra of (*B*) a non-diabetic and (*C*) a diabetic mouse at 5 weeks post-TAC. (*D*) Cardiac PCr/ATP ratio. Data are means ± SD (n = 6–8 for non-diabetic mice, n = 5–7 for diabetic mice). $^{*}P < 0.05$ vs. non-diabetic mice at the same time point, $^{\#}P < 0.05$ vs. baseline for the same genotype, $^{\ddagger}P < 0.05$ vs. 1 week post-TAC for the same genotype, $^{\wedge}P < 0.05$ vs. 5 weeks post-TAC for the same genotype.

electron transfer flavoprotein alpha and beta subunit (ETFA and ETFB), very long-chain acyl-CoA dehydrogenase (VLCAD), short-chain enoyl-CoA hydratase (ECHS1), medium and short-chain L-3-hydroxyacyl-coenzyme A dehydrogenase (HADH), hydroxyacyl-CoA dehydrogenase/3-ketoacyl-CoA thiolase/enoyl-CoA hydratase (trifunctional protein) beta subunit (HADHB), enoyl-CoA delta isomerase 1 (ECI1)] independent of genotype (general TAC effect $P < 0.01$). Also, expression of TCA cycle components [citrate synthase (CS), isocitrate dehydrogenase 3 (NAD(+)) alpha (IDH3A), oxoglutarate dehydrogenase (OGDH), dihydrolipoamide S-succinyltransferase (DLST), succinate-CoA ligase alpha subunit (SUCLG1), succinate-CoA ligase ADP-forming beta subunit (SUCLA2), fumarate hydratase 1 (FH1), malate dehydrogenase 2 (MDH2), solute carrier family 25 member 10 (SLC25A10), SLC25A11, and SLC25A22] and oxidative phosphorylation proteins [mitochondrially encoded NADH (MTND5), NADH:ubiquinone oxidoreductase core subunit S1 (NDUFS1), succinate dehydrogenase complex flavoprotein subunit A (SDHA), ubiquinol-cytochrome C reductase core protein II (UQCRC2), ATP synthase subunit beta (ATP5b)] was decreased upon TAC. Furthermore, expression of the pyruvate dehydrogenase (PDH) complex enzymes [PDH (lipoamide) alpha 1 (PDHA1), dihydrolipoamide s-acetyltransferase (DLAT)] was significantly decreased at 12 weeks after TAC as compared with baseline. Effects of diabetes were found on the expression of a few proteins. The expression of VLCAD was higher in diabetic as compared with non-diabetic mice (general genotype effect $P = 0.002$), while the expression of pyruvate dehydrogenase kinase 1 (PDK1), SLC25A1, SLC25A11, and MTND5 was lower compared with non-diabetic mice (general genotype effect $P < 0.05$).

Taken together, from a proteomics perspective, an overall downregulation of all steps of mitochondrial metabolism after TAC appears to contribute to the observed decrease in mitochondrial oxidative capacity in both non-diabetic and diabetic hearts.

3.9 TAC normalized the phosphorylation level of acetyl-CoA carboxylase in diabetic mice to the baseline levels of non-diabetic mice

To investigate the mechanism underlying the better maintenance of FAO capacity in the diabetic mice after TAC, we measured p-ACC at baseline and 12 weeks post-TAC. Consistent with the higher mitochondrial capacity of diabetic mice to oxidize FA, the *ex vivo* western blot analysis (*Figure 7A, B*) showed higher p-ACC levels and thus increased inhibition of activity of ACC, an enzyme catalyzing the formation of malonyl-CoA, in diabetic mice as compared with non-diabetic mice (general genotype effect $P = 0.009$). Total ACC was similar between diabetic and non-diabetic mice, and was not affected by TAC (*Figure 7C*).

3.10 Hypertrophic signalling pathways

We also studied signalling pathways known to be involved in hypertrophy: the mTOR,[25–28] mitogen-activated protein kinase (MAPK)/ERK,[29] PKD1[30,31] and CAMKII[32]. In this study, 12 weeks of TAC did not affect the phosphorylation degree of mTOR (*Figure 7D*) or ERK (*Figure 7E*), and increased the phosphorylation of CAMKII (general TAC effect: $P = 0.011$; *Figure 7F*). However, no genotype effects were found on any of these proteins. On the other hand, while the phosphorylation of PKD1 also increased upon TAC (general TAC effect: $P = 0.022$), it was lower in diabetic mice than in non-diabetic mice (general genotype effect: $P = 0.018$; *Figure 7G*). The level of phosphorylated PKD1 in diabetic mice at 12 weeks post-TAC was also similar to the level in non-diabetic mice at baseline. Total PKD1 expression was not changed (*Figure 7H*). PKD1, previously classified as PKC-μ, has been suggested to be involved in the development of cardiac hypertrophy through the PKD1-HDAC5-MEF2 signalling pathway[33] or through direct effects on glucose uptake.[34] We therefore further explored PKD's downstream targets, i.e. troponin I

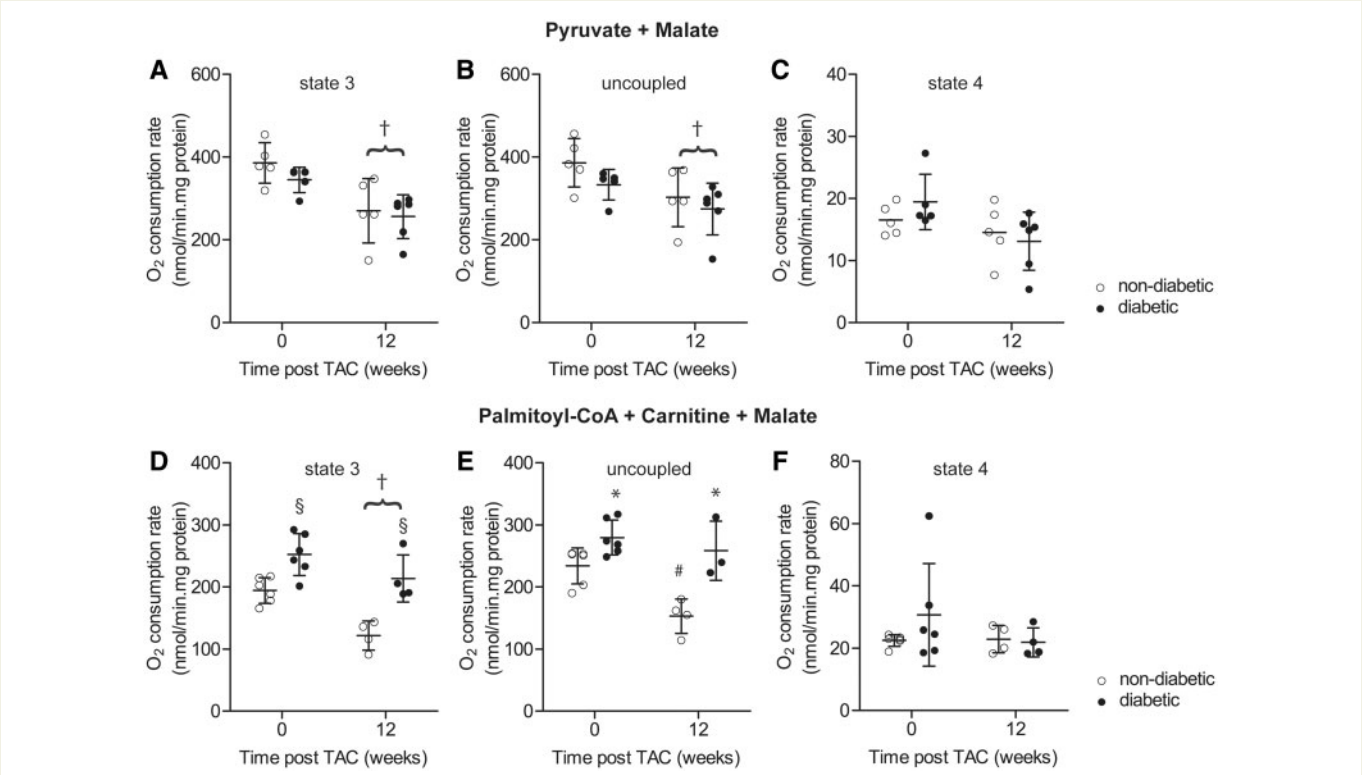

Figure 5 TAC decreased cardiac mitochondrial oxidative capacity, but FAO capacity was better maintained in diabetic mice. State 3, uncoupled, and state 4 respiration when (*A–C*) pyruvate plus malate or (*D–F*) palmitoyl-CoA plus carnitine plus malate were used as substrates. Data are means ± SD (n = 4–6 per group). $^{\dagger}P < 0.05$ vs. baseline independent of genotype, $^{\S}P < 0.05$ vs. non-diabetic mice independent of time, $^{*}P < 0.05$ vs. non-diabetic mice at the same time point, $^{\#}P < 0.05$ vs. baseline for the same genotype.

and HDAC5. Similar to PKD1 phosphorylation, cardiac troponin-I phosphorylation was increased 12 weeks post-TAC as compared with baseline (general TAC effect: $P < 0.01$; see Supplementary material online, *Figure S3B*), and tended to be lower in diabetic mice (general genotype effect: $P = 0.08$). However, HDAC5 phosphorylation was not significantly increased upon TAC (see Supplementary material online, *Figure S3C*) and also no genotype effect was detected on the phosphorylation level of HDAC5.

To further explore possible re-activation of the fetal gene program, we measured mRNA levels of the natriuretic peptides BNP and ANF. Although there was an increase in BNP gene expression upon TAC (general TAC effect: $P = 0.01$; see Supplementary material online, *Figure S3D*), the diabetic mice had reduced expression of BNP (general genotype effect: $P = 0.01$). ANF gene expression was not changed upon TAC or upon diabetes (see Supplementary material online, *Figure S3E*).

4. Discussion

Here we present the first comprehensive, longitudinal *in vivo* investigation of short- and long-term cardiac metabolic, structural, and functional changes in non-diabetic and diabetic mice during a time frame of 12 weeks after the induction of pressure overload. The *in vivo* measurements were complemented with *ex vivo* high-resolution respirometry, proteomics, western blotting, and quantitative PCR to elucidate the underlying molecular pathways. We observed that in non-diabetic mice, TAC induced cardiac hypertrophy and dysfunction, which was strongly correlated with increased myocardial glucose uptake. TAC also increased the levels of phosphorylated PKD1. Myocardial glucose uptake was increased already early in the development of heart failure in these mice and preceded a decrease in cardiac energy status. In comparison to non-diabetic mice, diabetic mice showed lower myocardial glucose uptake, lower cardiac energy status, and an increased mitochondrial capacity to oxidize FA at baseline. Unexpectedly, TAC affected cardiac function only mildly in diabetic mice within the 12 week time frame after TAC surgery. Also, the increase in LV mass upon TAC was much less pronounced in diabetic mice than in non-diabetic mice. The mild effect of TAC in diabetic mice was accompanied by a normalization of myocardial glucose uptake and the levels of phosphorylated PKD1 to the values of non-diabetic mice at baseline. In addition, the diabetic mice showed a blunted reduction in *ex vivo* mitochondrial capacity for FAO and a normalization of cardiac energy status at 12 weeks post-TAC. Our data suggest that in diabetic mice myocardial substrate balance is restored upon pressure overload, and that this in turn protects them from pressure overload induced heart failure.

4.1 (Mal-)adaptive cardiac metabolic switch towards increased glucose uptake upon pressure overload

The increase in myocardial glucose uptake during heart failure development as observed in this study is in agreement with previous reports showing that increased glucose utilization occurs early in heart failure (reviewed in[35]). However, it has not been clear whether the metabolic

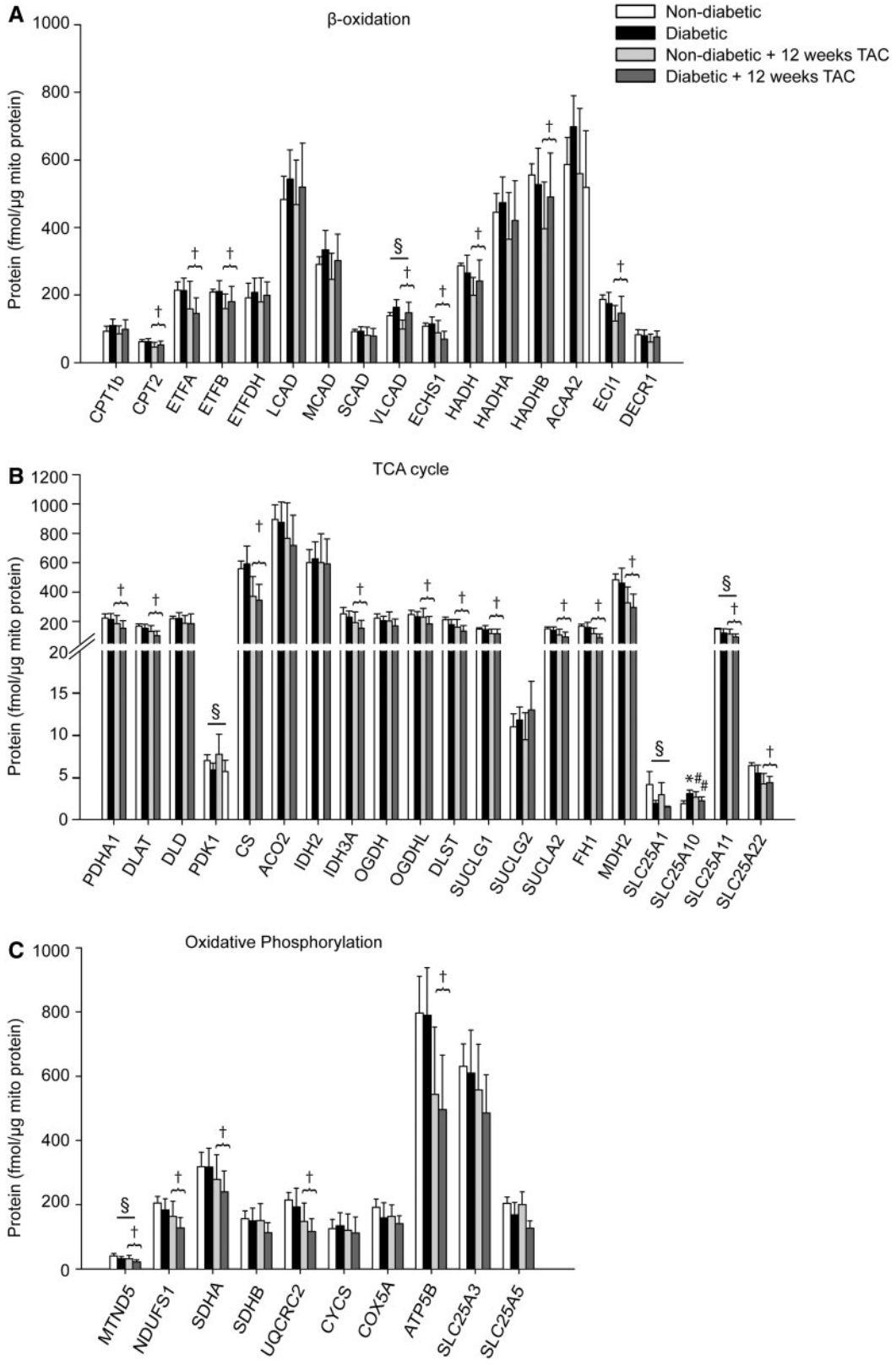

Figure 6 TAC lowered levels of mitochondrial proteins involved in FAO, TCA cycle and oxidative phosphorylation. Targeted quantitative proteomics of proteins involved in (*A*) β-oxidation, (*B*) TCA cycle, and (*C*) oxidative phosphorylation. Data are means ± SD (n = 5–6 per group). $^{\dagger}P < 0.05$ vs. baseline independent of genotype, $^{\S}P < 0.05$ vs. non-diabetic mice independent of time, $^{*}P < 0.05$ vs. non-diabetic mice at the same time point, $^{\#}P < 0.05$ vs. baseline for the same genotype. The list of abbreviation of the proteins is given in Supplementary material online, *Table S2*.

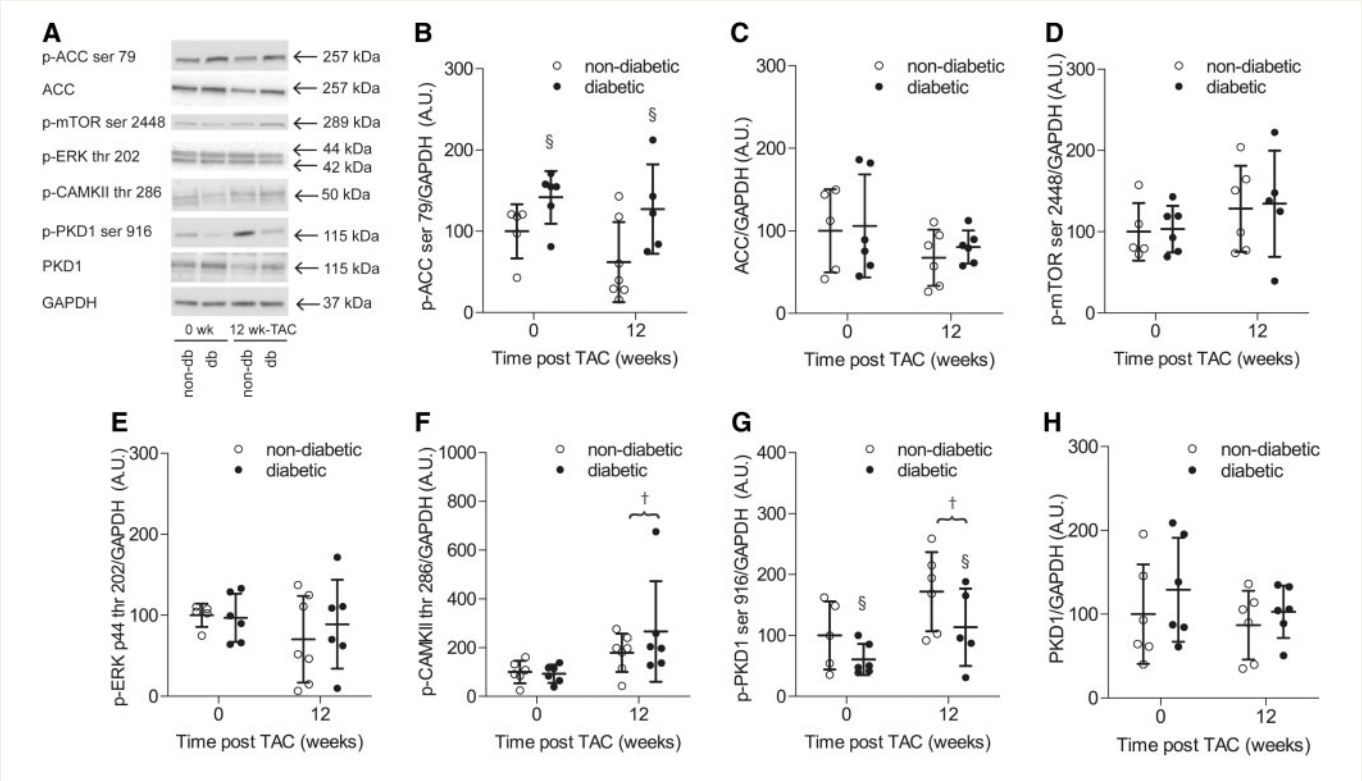

Figure 7 TAC and diabetes induce specific signalling pathways. Representative immunoblot images (*A*), and quantification of (*B*) p-ACC, (*C*) total ACC, (*D*) p-mTOR, (*E*) p-ERK, (*F*) p-CAMKII, (*G*) p-PKD1, and (*H*) total PKD1 protein expression. Data are GAPDH-normalized and are means ± SD (n = 5–7 per group). $^{\dagger}P < 0.05$ vs. baseline independent of genotype, $^{\S}P < 0.05$ vs. non-diabetic mice independent of time.

shift towards increased glucose utilization during the development of heart failure is an adaptive, or rather a detrimental mechanism. If the increased myocardial glucose uptake was an adaptive response to the increased workload, the correlation between myocardial glucose uptake and the severity of cardiac dysfunction in our non-diabetic mice indicates that this compensatory mechanism still could not prevent the progression towards heart failure. Indeed, previous studies have shown that the hypertrophied heart seems to be unable to increase glucose utilization to the levels required to maintain function,[2,4] and further stimulation of glucose utilization is necessary to rescue the heart upon pressure overload.[13] On the other hand, preventing an increase in glucose uptake upon TAC by propranolol was shown to protect the heart from failing,[6] suggesting that the shift towards increased glucose utilization is maladaptive.

Increased glucose uptake may not be beneficial when it is not matched with a sufficient increase in glucose oxidation, which could be the case in heart failure because of decreased mitochondrial function. Previous studies have shown reduced mitochondrial oxidative capacity upon heart failure in isolated heart mitochondria and permeabilized cardiac fibres of dogs[36,37] and patients.[38,39] It has been shown that the mismatch between glucose uptake and glucose oxidation results in the accumulation of glucose-6-phosphate, which activates mTOR and in turn induces cardiac hypertrophy.[28,35] Our study shows a downregulation of mitochondrial proteins as well as a reduced *ex vivo* mitochondrial capacity to oxidize glucose-derived substrates at 12 weeks post-TAC in both non-diabetic and diabetic mice. These data indicate that the increase in glucose uptake may not have been matched by a sufficient capacity for glucose oxidation, in particular in non-diabetic mice.

In diabetic mice, however, the TAC-induced increase in myocardial glucose uptake was much lower than in non-diabetic mice and myocardial glucose uptake was in fact normalized to the baseline values of non-diabetic mice. Together with the observation that the levels of mitochondrial proteins and oxidative capacity for glucose-derived substrates were similar between non-diabetic and diabetic mice upon TAC, this may suggest a better matching between glucose uptake and oxidation in the diabetic hearts upon TAC. This, in turn, can be linked with the less pronounced LV hypertrophy in diabetic mice compared with non-diabetic mice; however, in this study, pressure overload-induced LV hypertrophy was not associated with any significant changes in phosphorylated mTOR, suggesting that other pathways leading to hypertrophy are involved.

Another protein that may be involved in hypertrophic signalling is PKD1.[40] Pressure overload induces endothelin production,[41] which in turn activates protein kinase C (PKC) in tissues including heart, resulting in PKC-induced PKD1 activation and phosphorylation.[42] PKD1 overexpression has been associated with increased phosphorylation of HDAC5,[43] and subsequently, transcription of hypertrophic genes regulated by hypertrophic transcription factor MEF2.[40] In addition, PKD1 phosphorylation has previously been shown to induce GLUT4 translocation to the sarcolemma, and consequently, increase glucose uptake.[30,31] Increased glucose uptake has also been linked to hypertrophy.[44] In this study, TAC led to increased levels of phosphorylated PKD1 in both non-diabetic and diabetic mice, but the levels were consistently lower in the diabetic mice. These data are in agreement with the increased myocardial glucose uptake and hypertrophy upon TAC in the non-diabetic mice, and the overall lower glucose uptake and attenuated hypertrophy

in the diabetic mice. Interestingly, like our diabetic mice, PKD1 knockout mice also show inhibited hypertrophy and better cardiac function in response to pressure overload.[40] Additionally, decreased PKD1 phosphorylation was shown to be involved in the protection against long-term pressure overload in scaffold protein muscle A-kinase anchoring protein β knockout mice.[45] Lower PKD1 phosphorylation in the diabetic mice could therefore explain the protection against pressure overload-induced hypertrophy and impairment in function. Yet, this PKD1 involvement does not seem to proceed via the classical PKD1-HDAC5-MEF2 axis, given that HDAC5 phosphorylation was not significantly increased upon TAC and was also not lower in diabetic mice compared with non-diabetic mice. More likely, PKD1 thus affects hypertrophy through its direct effects on glucose uptake, resulting in a return to the fetal gene program. Future research is however required to elucidate the link between PKD1 and pressure overload-induced changes in cardiac metabolism, structure, and function.

4.2 High FA metabolism in diabetic mice

The diabetic heart primarily relies on FA utilization for energy production.[46,47] The higher ACC phosphorylation in the diabetic hearts as compared with non-diabetic hearts in this study suggests decreased malonyl-CoA formation and therefore less inhibition of CPT1b and higher mitochondrial FA uptake in the diabetic hearts. The protein levels of VLCAD, an enzyme involved in FA β-oxidation, were also increased in cardiac mitochondria of diabetic mice, indicating increased FAO. Additionally, the higher myocardial lipid content, higher *ex vivo* mitochondrial oxidative capacity for FA-derived substrates, and lower myocardial glucose uptake support that the diabetic mice rely more on FA as a substrate for oxidation than on glucose. Although TAC suppressed *ex vivo* mitochondrial oxidative capacity for FA-derived substrates in non-diabetic mice, the mitochondrial oxidative capacity for FA-derived substrates (in the uncoupled state) was maintained in diabetic mice. Therefore, we speculate that, although TAC led to decreased expression of mitochondrial proteins involved in oxidative metabolism in both non-diabetic and diabetic mice, the maintained mitochondrial capacity to oxidize FA in the diabetic mice may be sufficient to preserve cardiac function upon pressure overload, which is in agreement with a previous study in diabetic and high-fat diet fed mice.[48] This hypothesis is further corroborated by the observation that other mouse models with increased FAO, such as cardiac specific ACC2 knockout mice,[3] were also protected from heart failure upon TAC[3] and Angiotensin-induced pressure overload.[49] Furthermore, it was shown that reducing myocardial FA utilization through ablation of FAT/CD36 or CPT1b, proteins involved in FA transport over the cellular and mitochondrial membranes, respectively, resulted in exacerbated cardiac dysfunction and energetic impairment after TAC.[18,19]

4.3 Restoration of substrate balance upon pressure overload in diabetic mice

Although the increased reliance on FA metabolism in diabetic mice has actually been linked with detrimental effects related to diabetic cardiomyopathy (reviewed in[50]), our data suggest that pressure overload restored the myocardial substrate balance[51] in diabetic mice. Twelve weeks of TAC increased myocardial glucose uptake and PKD1 phosphorylation in diabetic mice to the baseline levels of non-diabetic mice. The restoration of the substrate balance in the diabetic heart could therefore explain why cardiac function was largely maintained in diabetic mice. Interestingly, cardiac energy status in diabetic mice even increased at 12 weeks post-TAC as compared with baseline and 1 week post-TAC. In the non-diabetic mice, the increase in glucose uptake and suppression of FAO upon TAC disturbed the substrate balance and shifted it towards increased dependence on glucose utilization. The importance of maintaining the substrate balance has previously been demonstrated in mice with cardiac-specific PKD1 overexpression.[30] PKD1 overexpressing mice show a shift towards increased glucose utilization, which is paralleled by cardiac hypertrophy and ventricular dilatation.[30] However, feeding PKD1 overexpressing mice a high fat diet normalized cardiac morphology and function.[30]

Our observation that diabetic mice were protected against pressure overload, while surprising, is in line with the concept of the 'obesity paradox' in obese heart failure patients. Despite the increased risk of heart failure in obese patients, the prognosis for obese heart failure patients is actually better than that for non-obese heart failure patients.[23] We propose that the restoration of substrate balance could explain this phenomenon.

4.4 Reduced cardiac energy status as an effect of heart failure progression

A reduced PCr/ATP ratio in the failing heart has been reported in both animals[52,53] and patients,[8,54] and cardiac energy status was shown to be a strong predictor of mortality in heart failure patients.[8] Our data show, however, that the decreased cardiac function in non-diabetic mice, which was already present at 1 week post-TAC, is unlikely to be explained by an impairment of cardiac energetics, as we observed a reduction in the PCr/ATP ratio only at 12 weeks after TAC. Therefore, reduced cardiac energy status rather seems to be an effect of heart failure progression, and may only become prominent when total mitochondrial oxidative metabolism has declined. Furthermore, from the observation that cardiac function of diabetic mice was normal at baseline and was maintained upon TAC despite their low cardiac energy status, which was not recovered until 12 weeks post-TAC, we can conclude that low cardiac energy status does not play a decisive role in the development of heart failure in mice. We suggest that the lack of functional consequences of the low cardiac PCr/ATP ratio in diabetic mice may be explained by a compensatory increase in the forward creatine kinase reaction rate to maintain ATP supply, as shown in a previous study in Zucker diabetic rats.[55]

4.5 Limitation of the study

A limitation of this study is the lack of leptin signalling in the *db/db* mouse model due to leptin receptor deficiency. Obesity is associated with hyperleptinemia. In obese subjects, high levels of circulating leptin have been correlated with cardiac hypertrophy, but animal studies have not supported a role for leptin in promoting cardiac hypertrophy.[56] As the role of leptin in cardiac remodelling remains unclear, one has to consider the lack of leptin signalling in *db/db* mice when translating our finding to other, non-genetic models of diabetes or to the human situation.

4.6 Concluding remarks

Taken together, this study provides the first longitudinal *in vivo* data of cardiac metabolic, energetic, structural, and functional adaptations during heart failure development and progression in non-diabetic and diabetic mice. Our data show that the development of heart failure in non-diabetic mice was correlated with increased PKD1 phosphorylation and increased myocardial glucose uptake, which preceded the decrease in cardiac energy status. Although diabetic mice showed lower PKD1

phosphorylation and glucose uptake than non-diabetic mice at baseline, these values were normalized upon TAC. The mild cardiac hypertrophy, preserved function, and recovered energy status in diabetic mice upon pressure overload therefore suggest that maintenance of myocardial substrate balance is beneficial for cardiac function in pressure overload-induced heart failure. Phenotyping of cardiac substrate metabolism may thus guide the diagnosis and treatment of patients with pressure overload-induced hypertrophy and improve clinical outcomes.

Supplementary material

Supplementary material is available at *Cardiovascular Research* online.

Acknowledgements

We thank Leonie Niesen, Dirk Reinhardt, David Veraart, Sarah Koester, Roman Priebe, Nina Nagelmann, and Justina Wolters for expert technical assistance.

Conflict of interest: none declared.

Funding

D.A. and J.J.P. are supported by a Vidi grant (project: 700.58.421) and M.N. is supported by a Veni grant (project: 916.14.050) from the Netherlands Organization for Scientific Research (NWO). D.A. is also supported by a travel grant from the Boehringer Ingelheim Fonds to perform the experiments in Münster. This work was partly supported by the Deutsche Forschungsgemeinschaft, Collaborative Research Center SFB 656 'Cardiovascular Molecular Imaging', project Z2 and by the Interdisciplinary Centre for Clinical Research (IZKF, core unit PIX), Münster, Germany.

References

1. Ingwall JS. Energy metabolism in heart failure and remodelling. *Cardiovasc Res* 2009;**81**:412–419.
2. Pereira RO, Wende AR, Olsen C, Soto J, Rawlings T, Zhu Y, Anderson SM, Abel ED. Inducible overexpression of GLUT1 prevents mitochondrial dysfunction and attenuates structural remodeling in pressure overload but does not prevent left ventricular dysfunction. *J Am Heart Assoc* 2013;**2**:e000301.
3. Kolwicz SC, Jr., Olson DP, Marney LC, Garcia-Menendez L, Synovec RE, Tian R. Cardiac-specific deletion of acetyl CoA carboxylase 2 prevents metabolic remodeling during pressure-overload hypertrophy. *Circ Res* 2012;**111**:728–738.
4. Allard MF, Schonekess BO, Henning SL, English DR, Lopaschuk GD. Contribution of oxidative metabolism and glycolysis to ATP production in hypertrophied hearts. *Am J Physiol* 1994;**267**:H742–H750.
5. Christe ME, Rodgers RL. Altered glucose and fatty acid oxidation in hearts of the spontaneously hypertensive rat. *J Mol Cell Cardiol* 1994;**26**:1371–1375.
6. Zhong M, Alonso CE, Taegtmeyer H, Kundu BK. Quantitative PET imaging detects early metabolic remodeling in a mouse model of pressure-overload left ventricular hypertrophy in vivo. *J Nucl Med* 2013;**54**:609–615.
7. Hansch A, Rzanny R, Heyne JP, Leder U, Reichenbach JR, Kaiser WA. Noninvasive measurements of cardiac high-energy phosphate metabolites in dilated cardiomyopathy by using ^{31}P spectroscopic chemical shift imaging. *Eur Radiol* 2005;**15**:319–323.
8. Neubauer S, Horn M, Cramer M, Harre K, Newell JB, Peters W, Pabst T, Ertl G, Hahn D, Ingwall JS, Kochsiek K. Myocardial phosphocreatine-to-ATP ratio is a predictor of mortality in patients with dilated cardiomyopathy. *Circulation* 1997;**96**:2190–2196.
9. Nichols GA, Gullion CM, Koro CE, Ephross SA, Brown JB. The incidence of congestive heart failure in type 2 diabetes: an update. *Diabetes Care* 2004;**27**:1879–1884.
10. Oakes ND, Thalen P, Aasum E, Edgley A, Larsen T, Furler SM, Ljung B, Severson D. Cardiac metabolism in mice: tracer method developments and in vivo application revealing profound metabolic inflexibility in diabetes. *Am J Physiol Endocrinol Metab* 2006;**290**:E870–E881.
11. Scheuermann-Freestone M, Madsen PL, Manners D, Blamire AM, Buckingham RE, Styles P, Radda GK, Neubauer S, Clarke K. Abnormal cardiac and skeletal muscle energy metabolism in patients with type 2 diabetes. *Circulation* 2003;**107**:3040–3046.
12. Diamant M, Lamb HJ, Groeneveld Y, Endert EL, Smit JW, Bax JJ, Romijn JA, de Roos A, Radder JK. Diastolic dysfunction is associated with altered myocardial metabolism in asymptomatic normotensive patients with well-controlled type 2 diabetes mellitus. *J Am Coll Cardiol* 2003;**42**:328–335.
13. Liao R, Jain M, Cui L, D'agostino J, Aiello F, Luptak I, Ngoy S, Mortensen RM, Tian R. Cardiac-specific overexpression of GLUT1 prevents the development of heart failure attributable to pressure overload in mice. *Circulation* 2002;**106**:2125–2131.
14. Kienesberger PC, Pulinilkunnil T, Sung MM, Nagendran J, Haemmerle G, Kershaw EE, Young ME, Light PE, Oudit GY, Zechner R, Dyck JR. Myocardial ATGL overexpression decreases the reliance on fatty acid oxidation and protects against pressure overload-induced cardiac dysfunction. *Mol Cell Biol* 2012;**32**:740–750.
15. Luptak I, Balschi JA, Xing Y, Leone TC, Kelly DP, Tian R. Decreased contractile and metabolic reserve in peroxisome proliferator–activated receptor-α–null hearts can be rescued by increasing glucose transport and utilization. *Circulation* 2005;**112**:2339–2346.
16. Labinskyy V, Bellomo M, Chandler MP, Young ME, Lionetti V, Qanud K, Bigazzi F, Sampietro T, Stanley WC, Recchia FA. Chronic activation of peroxisome proliferator-activated receptor-alpha with fenofibrate prevents alterations in cardiac metabolic phenotype without changing the onset of decompensation in pacing-induced heart failure. *J Pharmacol Exp Ther* 2007;**321**:165–171.
17. Christopher BA, Huang HM, Berthiaume JM, McElfresh TA, Chen X, Croniger CM, Muzic RF, Jr, Chandler MP. Myocardial insulin resistance induced by high fat feeding in heart failure is associated with preserved contractile function. *Am J Physiol Heart Circ Physiol* 2010;**299**:H1917–H1927.
18. He L, Kim T, Long Q, Liu J, Wang P, Zhou Y, Ding Y, Prasain J, Wood PA, Yang Q. Carnitine palmitoyltransferase-1b deficiency aggravates pressure overload-induced cardiac hypertrophy caused by lipotoxicity. *Circulation* 2012;**126**:1705–1716.
19. Steinbusch LK, Luiken JJ, Vlasblom R, Chabowski A, Hoebers NT, Coumans WA, Vroegrijk IO, Voshol PJ, Ouwens DM, Glatz JF, Diamant M. Absence of fatty acid transporter CD36 protects against Western-type diet-related cardiac dysfunction following pressure overload in mice. *Am J Physiol Endocrinol Metab* 2011;**301**:E618–E627.
20. Arany Z, Novikov M, Chin S, Ma Y, Rosenzweig A, Spiegelman BM. Transverse aortic constriction leads to accelerated heart failure in mice lacking PPAR-g coactivator 1a. *Proc Natl Acad Sci U S A* 2006;**103**:10086–10091.
21. Augustus AS, Buchanan J, Park TS, Hirata K, Noh HL, Sun J, Homma S, D'armiento J, Abel ED, Goldberg IJ. Loss of lipoprotein lipase-derived fatty acids leads to increased cardiac glucose metabolism and heart dysfunction. *J Biol Chem* 2006;**281**:8716–8723.
22. Abdurrachim D, Luiken JJ, Nicolay K, Glatz JF, Prompers JJ, Nabben M. Good and bad consequences of altered fatty acid metabolism in heart failure: evidence from mouse models. *Cardiovasc Res* 2015;**106**:194–205.
23. Lavie CJ, Alpert MA, Arena R, Mehra MR, Milani RV, Ventura HO. Impact of obesity and the obesity paradox on prevalence and prognosis in heart failure. *JACC Heart Fail* 2013;**1**:93–102.
24. van Nierop BJ, van Assen HC, van Deel ED, Niesen LB, Duncker DJ, Strijkers GJ, Nicolay K. Phenotyping of left and right ventricular function in mouse models of compensated hypertrophy and heart failure with cardiac MRI. *PLoS One* 2013;**8**:e55424.
25. Shioi T, McMullen JR, Tarnavski O, Converso K, Sherwood MC, Manning WJ, Izumo S. Rapamycin attenuates load-induced cardiac hypertrophy in mice. *Circulation* 2003;**107**:1664–1670.
26. Boluyt MO, Li ZB, Loyd AM, Scalia AF, Cirrincione GM, Jackson RR. The mTOR/p70S6K signal transduction pathway plays a role in cardiac hypertrophy and influences expression of myosin heavy chain genes in vivo. *Cardiovasc Drugs Ther* 2004;**18**:257–267.
27. McMullen JR, Sherwood MC, Tarnavski O, Zhang L, Dorfman AL, Shioi T, Izumo S. Inhibition of mTOR signaling with rapamycin regresses established cardiac hypertrophy induced by pressure overload. *Circulation* 2004;**109**:3050–3055.
28. Sen S, Kundu BK, Wu HC, Hashmi SS, Guthrie P, Locke LW, Roy RJ, Matherne GP, Berr SS, Terwelp M, Scott B, Carranza S, Frazier OH, Glover DK, Dillmann WH, Gambello MJ, Entman ML, Taegtmeyer H. Glucose regulation of load-induced mTOR signaling and ER stress in mammalian heart. *J Am Heart Assoc* 2013;**2**:e004796.
29. Takeishi Y, Huang Q, Abe J, Glassman M, Che W, Lee JD, Kawakatsu H, Lawrence EG, Hoit BD, Berk BC, Walsh RA. Src and multiple MAP kinase activation in cardiac hypertrophy and congestive heart failure under chronic pressure-overload: comparison with acute mechanical stretch. *J Mol Cell Cardiol* 2001;**33**:1637–1648.
30. Dirkx E, van Eys GJ, Schwenk RW, Steinbusch LK, Hoebers N, Coumans WA, Peters T, Janssen BJ, Brans B, Vogg AT, Neumann D, Glatz JF, Luiken JJ. Protein kinase-D1 overexpression prevents lipid-induced cardiac insulin resistance. *J Mol Cell Cardiol* 2014;**76**:208–217.
31. Harrison BC, Kim MS, van Rooij E, Plato CF, Papst PJ, Vega RB, McAnally JA, Richardson JA, Bassel-Duby R, Olson EN, McKinsey TA. Regulation of cardiac stress signaling by protein kinase D1. *Mol Cell Biol* 2006;**26**:3875–3888.
32. Anderson ME, Brown JH, Bers DM. CaMKII in myocardial hypertrophy and heart failure. *J Mol Cell Cardiol* 2011;**51**:468–473.
33. Olson EN, Backs J, McKinsey TA. Control of cardiac hypertrophy and heart failure by histone acetylation/deacetylation. *Novartis Found Symp* 2006;**274**:3–12. discussion 13-19, 152-155, 272-156.
34. van Bilsen M, Smeets PJ, Gilde AJ, van der Vusse GJ. Metabolic remodelling of the failing heart: the cardiac burn-out syndrome?. *Cardiovasc Res* 2004;**61**:218–226.
35. Kundu BK, Zhong M, Sen S, Davogustto G, Keller SR, Taegtmeyer H. Remodeling of glucose metabolism precedes pressure overload-induced left ventricular hypertrophy: review of a hypothesis. *Cardiology* 2015;**130**:211–220.

36. Sharov VG, Goussev A, Lesch M, Goldstein S, Sabbah HN. Abnormal mitochondrial function in myocardium of dogs with chronic heart failure. *J Mol Cell Cardiol* 1998;**30**:1757–1762.
37. Rosca MG, Vazquez EJ, Kerner J, Parland W, Chandler MP, Stanley W, Sabbah HN, Hoppel CL. Cardiac mitochondria in heart failure: decrease in respirasomes and oxidative phosphorylation. *Cardiovasc Res* 2008;**80**:30–39.
38. Lemieux H, Semsroth S, Antretter H, Hofer D, Gnaiger E. Mitochondrial respiratory control and early defects of oxidative phosphorylation in the failing human heart. *Int J Biochem Cell Biol* 2011;**43**:1729–1738.
39. Sharov VG, Todor AV, Silverman N, Goldstein S, Sabbah HN. Abnormal mitochondrial respiration in failed human myocardium. *J Mol Cell Cardiol* 2000;**32**:2361–2367.
40. Fielitz J, Kim MS, Shelton JM, Qi X, Hill JA, Richardson JA, Bassel-Duby R, Olson EN. Requirement of protein kinase D1 for pathological cardiac remodeling. *Proc Natl Acad Sci U S A* 2008;**105**:3059–3063.
41. Yorikane R, Sakai S, Miyauchi T, Sakurai T, Sugishita Y, Goto K. Increased production of endothelin-1 in the hypertrophied rat heart due to pressure overload. *FEBS Lett* 1993;**332**:31–34.
42. Haworth RS, Roberts NA, Cuello F, Avkiran M. Regulation of protein kinase D activity in adult myocardium: novel counter-regulatory roles for protein kinase Ce and protein kinase A. *J Mol Cell Cardiol* 2007;**43**:686–695.
43. Huynh QK, McKinsey TA. Protein kinase D directly phosphorylates histone deacetylase 5 via a random sequential kinetic mechanism. *Arch Biochem Biophys* 2006;**450**:141–148.
44. Kolwicz SC, Jr, Tian R. Glucose metabolism and cardiac hypertrophy. *Cardiovasc Res* 2011;**90**:194–201.
45. Kritzer MD, Li J, Passariello CL, Gayanilo M, Thakur H, Dayan J, Dodge-Kafka K, Kapiloff MS. The scaffold protein muscle A-kinase anchoring protein beta orchestrates cardiac myocyte hypertrophic signaling required for the development of heart failure. *Circ Heart Fail* 2014;**7**:663–672.
46. Aasum E, Belke DD, Severson DL, Riemersma RA, Cooper M, Andreassen M, Larsen TS. Cardiac function and metabolism in type 2 diabetic mice after treatment with BM 17.0744, a novel PPAR-a activator. *Am J Physiol Heart Circ Physiol* 2002;**283**: H949–H957.
47. Mather KJ, Hutchins GD, Perry K, Territo W, Chisholm R, Acton A, Glick-Wilson B, Considine RV, Moberly S, DeGrado TR. Assessment of myocardial metabolic flexibility and work efficiency in human type 2 diabetes using 16-[^{18}F]fluoro-4-thiapalmitate, a novel PET fatty acid tracer. *Am J Physiol Endocrinol Metab* 2016;**310**:E452–E460.
48. Brainard RE, Watson LJ, Demartino AM, Brittian KR, Readnower RD, Boakye AA, Zhang D, Hoetker JD, Bhatnagar A, Baba SP, Jones SP. High fat feeding in mice is insufficient to induce cardiac dysfunction and does not exacerbate heart failure. *PLoS One* 2013;**8**:e83174.
49. Choi YS, de Mattos AB, Shao D, Li T, Nabben M, Kim M, Wang W, Tian R, Kolwicz SC. Jr., Preservation of myocardial fatty acid oxidation prevents diastolic dysfunction in mice subjected to angiotensin II infusion. *J Mol Cell Cardiol* 2016;**100**:64–71.
50. Zlobine I, Gopal K, Ussher JR. Lipotoxicity in obesity and diabetes-related cardiac dysfunction. *Biochim Biophys Acta* 2016;**1861**:1555–1568.
51. Glatz JF, Bonen A, Ouwens DM, Luiken JJ. Regulation of sarcolemmal transport of substrates in the healthy and diseased heart. *Cardiovasc Drugs Ther* 2006;**20**:471–476.
52. Gupta A, Chacko VP, Weiss RG. Abnormal energetics and ATP depletion in pressure-overload mouse hearts: in vivo high-energy phosphate concentration measures by non-invasive magnetic resonance. *Am J Physiol Heart Circ Physiol* 2009;**297**:H59–H64.
53. Maslov MY, Chacko VP, Stuber M, Moens AL, Kass DA, Champion HC, Weiss RG. Altered high-energy phosphate metabolism predicts contractile dysfunction and subsequent ventricular remodeling in pressure-overload hypertrophy mice. *Am J Physiol Heart Circ Physiol* 2007;**292**:H387–H391.
54. Hardy CJ, Weiss RG, Bottomley PA, Gerstenblith G. Altered myocardial high-energy phosphate metabolites in patients with dilated cardiomyopathy. *Am Heart J* 1991;**122**:795–801.
55. Bashir A, Coggan AR, Gropler RJ. In vivo creatine kinase reaction kinetics at rest and stress in type II diabetic rat heart. *Physiol Rep* 2015;**3**:
56. Hall ME, Harmancey R, Stec DE. Lean heart: Role of leptin in cardiac hypertrophy and metabolism. *World J Cardiol* 2015;**7**:511–524.